National Library of Canada
Bibliothèque nationale du Canada

Canadian Theses Service
Service des thèses canadiennes

Ottawa, Canada
K1A 0N4

NOTICE

The quality of this microform is heavily dependent upon the quality of the original thesis submitted for microfilming. Every effort has been made to ensure the highest quality of reproduction possible.

If pages are missing, contact the university which granted the degree.

Some pages may have indistinct print, especially if the original pages were typed with a poor typewriter ribbon or if the university sent us an inferior photocopy.

Previously copyrighted materials (journal articles, published tests, etc.) are not filmed.

Reproduction in full or in part of this microform is governed by the Canadian Copyright Act, R.S.C. 1970, c. C-30.

AVIS

La qualité de cette microforme dépend grandement de la qualité de la thèse soumise au microfilmage. Nous avons tout fait pour assurer une qualité supérieure de reproduction.

S'il manque des pages, veuillez communiquer avec l'université qui a conféré le grade.

La qualité d'impression de certaines pages peut laisser à désirer, surtout si les pages originales ont été dactylographiées à l'aide d'un ruban usé ou si l'université nous a fait parvenir une photocopie de qualité inférieure.

Les documents qui font déjà l'objet d'un droit d'auteur (articles de revue, tests publiés, etc.) ne sont pas microfilmés.

La reproduction, même partielle, de cette microforme est soumise à la Loi canadienne sur le droit d'auteur, SRC 1970, c. C-30.

NL-339 (r. 86/04)

Canada

THE UNIVERSITY OF ALBERTA

EFFECTS OF COVER ELECTRODE AND PREPARATION TECHNIQUE ON THE TUNNELING CHARACTERISTICS OF Mg - MgO - METAL JUNCTIONS

BY

© YUEBIN NING

A THESIS

SUBMITTED TO THE FACULTY OF GRADUATE STUDIES AND RESEARCH

IN PARTIAL FULFILMENT OF THE REQUIREMENTS FOR THE DEGREE

OF MASTER OF SCIENCE

IN

SOLID STATE PHYSICS

DEPARTMENT OF PHYSICS

EDMONTON, ALBERTA

FALL 1987

Permission has been granted to the National Library of Canada to microfilm this thesis and to lend or sell copies of the film.

The author (copyright owner) has reserved other publication rights, and neither the thesis nor extensive extracts from it may be printed or otherwise reproduced without his/her written permission.

L'autorisation a été accordée à la Bibliothèque nationale du Canada de microfilmer cette thèse et de prêter ou de vendre des exemplaires du film.

L'auteur (titulaire du droit d'auteur) se réserve les autres droits de publication; ni la thèse ni de longs extraits de celle-ci ne doivent être imprimés ou autrement reproduits sans son autorisation écrite.

ISBN 0-315-40928-2

THE UNIVERSITY OF ALBERTA

RELEASE FORM

NAME OF AUTHOR YUEBIN NING

TITLE OF THESIS EFFECTS OF COVER ELECTRODE AND PREPARATION TECHNIQUE ON THE TUNNELING CHARACTERISTICS OF Mg - MgO - METAL JUNCTIONS

DEGREE FOR WHICH THESIS WAS PRESENTED MASTER OF SCIENCE

YEAR THIS DEGREE GRANTED FALL 1987

Permission is hereby granted to THE UNIVERSITY OF ALBERTA LIBRARY to reproduce single copies of this thesis and to lend or sell such copies for private, scholarly or scientific research purposes only.

The author reserves other publication rights, and neither the thesis nor extensive extracts from it may be printed or otherwise reproduced without the author's written permission.

(SIGNED) ..... Yuebin Ning

PERMANENT ADDRESS:

c/o DEPARTMENT OF PHYSICS

THE UNIVERSITY OF ALBERTA

EDMONTON CANADA T6G 2J1

DATED September 1987

THE UNIVERSITY OF ALBERTA

FACULTY OF GRADUATE STUDIES AND RESEARCH

The undersigned certify that they have read, and recommend to the Faculty of Graduate Studies and Research, for acceptance, a thesis entitled EFFECTS OF COVER ELECTRODE AND PREPARATION TECHNIQUE ON THE TUNNELING CHARACTERISTICS OF Mg - MgO - METAL JUNCTIONS submitted by YUEBIN NING in partial fulfilment of the requirements for the degree of MASTER OF SCIENCE in SOLID STATE PHYSICS.

.....
Supervisor

.....

.....

.....
External Examiner

Date. 11th Sept. 1987.

Abstract

This thesis sets out to describe some of the effects of cover electrode and barrier preparation techniques on the tunneling characteristics of Mg - MgO - Metal junctions. In carrying out this investigation, various metals were used as cover electrodes of the tunnel junctions and different barrier preparation techniques were employed in forming the oxide tunnel barrier.

The influence of the cover electrode on the tunnel barrier properties and the Inelastic Electron Tunneling (IET) spectra are studied by detailed comparison of tunneling characteristics of junctions. Further insight into the nature of the influence is gained by varying the barrier preparation techniques.

The barrier height of the tunnel junctions is a function of the ionic radius of the cover electrode metal. Junctions with the Mg base film exposed to a flux of low energy hydrogen ions before oxidation exhibit a large barrier asymmetry and a large peak centered at 124 meV in the IET spectra. The observed hydroxyl stretch band is found to vary at about 450 meV with both the cover electrode material and sweep polarity. Possible mechanisms are discussed.

ACKOWLEDGEMENTS

I wish to express my gratitude to my supervisor, Dr. J. G. Adler, for his guidance throughout the course of this work. I also wish to thank him for providing funds which allowed me to attend a historic conference in New York.

My special thanks to my colleague, M. Gallagher, for his collaboration and help throughout the course of this work. His friendship and understanding have always been greatly appreciated.

Thanks are given to D. Mullin (FSCT) for many valuable technical assistances and help during the entire period of my stay in the laboratory. His tuition - free courses enriched my knowledge about a new culture and society in many many aspects, and made my life here easier.

Special acklowledgements are given to Dr. F. L. Weichman and Dr. Z. W. Gortel for much encouragement and many helpful discussions.

I wish to thank the Physics Department for its financial support. I would also like to thank the PRC for the scholarship which allowed me to come to Canada for graduate studies.

The help from Dr. B. S. Zheng during my writing of the thesis has been appreciated.

Finally, I would like to thank J. Straus and M. Konkin for some of the diagrams which appeare in this thesis.

TABLE OF CONTENTS

Chapter		Page
1.	INTRODUCTION	1
2.	THEORY	4
	2.1 Introduction	4
	2.2 Theory of elastic tunneling	8
	2.3 Theory of inelastic tunneling	12
3.	EXPERIMENTAL TECHNIQUES	20
	3.1 Junction preparation	20
	3.2 Formation of tunnel barriers	22
	3.3 Film thickness determination	24
	3.4 Measurement of tunneling characteristics	25
4.	DATA ANALYSIS	29
	4.1 Introduction	29
	4.2 Peak assignments	29
	4.3 Barrier parameters	32
	4.4 Peak intensity	33
5.	RESULTS AND DISCUSSION	35
	5.1 Introduction	35
	5.2 Barrier parameters	35
	5.3 IET spectra	40
	5.4 The O-H stretching peak	46
	5.5 Discussion of the 124 meV peak	55
6.	SUMMARY AND CONCLUSION	58
	6.1 Conclusion	58
	6.2 Suggestion for further work	59
BIBLIOGRAPHY		60

LIST OF TABLES

Table		Page
3.1	Evaporation materials	23
5.1	Barrier parameters	36
5.2	O-H peak intensities and positions	47
5.3	124 meV peak intensities and positions	56

LIST OF FIGURES

Figure		Page
2.1	Tunneling experiment	5
2.2	Energy level diagram for M - I - M junction	6
2.3	Schematic diagram for elastic and inelastic tunneling processes	13
2.4	I vs V, σ vs V, and $d\sigma/dV$ vs V	15
2.5	Interaction of tunneling electrons with a molecular vibrational mode	18
3.1	The tunnel junction layout	21
3.2	Layout of the bridge measuring system	26
4.1	Typical spectra of a plasma and a gun junction with a Pb cover electrode	30
5.1	Average barrier height Φ vs ionic radius of the cover electrode	38
5.2	Spectra for Mg - MgO - Metal junctions	41
5.3	E(O-H) in gun junctions vs the atomic radius of the cover metals	50
5.4	E(O-H) in gun junctions vs the percentage of d charater of the cover metals	53

1. INTRODUCTION

Inelastic electron tunneling spectroscopy (IETS) is a sensitive spectroscopic technique and has become established as a standard method for investigating various low - lying excitations in Metal Insulator - Metal systems in the last twenty years (Hansma 1982; Wolfram 1977). This unique technique has found fruitful applications in many areas including surface chemistry of molecular species absorbed on the oxide barrier, chemisorption on metal surfaces and the catalysis of oxidation.

In practice, barrier preparation and the choice of cover electrode are two major components in tunnel junction fabrication and crucial to IETS experiments. In the past, IETS experiments have mainly been carried out on Al - Al Oxide - Metal junctions , and the cover metals used were often limited to a few metals such as Pb and Al. Very little is known about the effect of the cover electrode on spectra and the barrier properties. A detailed understanding seems essential to further development of IETS technique and its applications. In previous studies, Magno et al. (Magno, Konkin and Adler 1977) studied the influence of cover electrodes on the IETS peak intensities in Al - Al oxide - Metal juctions. Kirtley and Hansma (Kirtley and Hansma 1975) reported the observation of an energy shift in the hydroxyl stretching (O-H) mode due to different cover electrodes. In this work, we extend previous studies to a consideration of

how different cover electrode materials and preparation techniques affect the properties of the underlying oxide which in turn affects the IET spectra.

The present work was carried out as a extension of previous work (Plesiewicz and Adler 1986) conducted in this laboratory on Mg - MgO - Pb junctions, with the initial hope of addressing some of the problems mentioned above. Data are shown for a series of Mg - MgO - M_x junctions where M_x is either Al, Ag, Au, Cd, Cu, In, Mg, Pb, Sn, or Zn. Barrier parameters of junctions prepared by two different methods are compared. We find that the pretreatment of the Mg base film with hydrogen ions drastically modifies the barrier properties. The barrier height of junctions is correlated to the ionic radius of the cover metal, and the correlation of the O-H stretching energy with the atomic radius and the percentage of d character of the cover metal will be presented. The dependence of this O-H stretching energy on sweep polarity will also be discussed. Finally, changes in the IET spectra due to the influence of the cover electrode is discussed.

The theory of electron tunneling, both elastic and inelastic, will be discussed along with a relatively simple mathematical treatment in Chapter 2. Junction preparation and the instrumentation used for measurement of junction properties will be described in Chapter 3. In Chapter 4, data handling and analysis will be discussed. In Chapter 5, results of the experiments will be presented along with

models and discussions based on the experimental data.

Finally, in the last chapter of the thesis, conclusions and suggestions for further work will be presented.

2. THEORY

2.1 Introduction

The concept of tunneling has come into existence since the inception of quantum mechanics. A particle represented by a wave funtion, may enter a classically forbidden region and, if the potential barrier is sufficiently thin, may tunnel through without having enough energy to go over the top of the barrier.

Physically, this concept can be realized in the form of a tunnel junction, in which electrons tunnel through an insulating barrier sandwiched between two metal electrodes. In Fig. 2.1, a typical description of a tunneling experiment is shown. Classically, if one attempts to apply a voltage across the junction, the result will simply be a charged capacitor, and no current will flow across the insulating barrier. Quantum mechanically however, a current flow can occur across this region provided that the insulating barrier is sufficiently thin. This is electron tunneling.

In order to understand the tunneling process, we start with the electron energy level diagram for metal - insulator - metal junction shown in Fig. 2.2. E_{F_1} and E_{F_2} are the Fermi levels of metal 1 and 2 respectively, while e is the electron charge and eV is the applied bias energy. Tunneling occurs from left to right across a barrier of thickness s

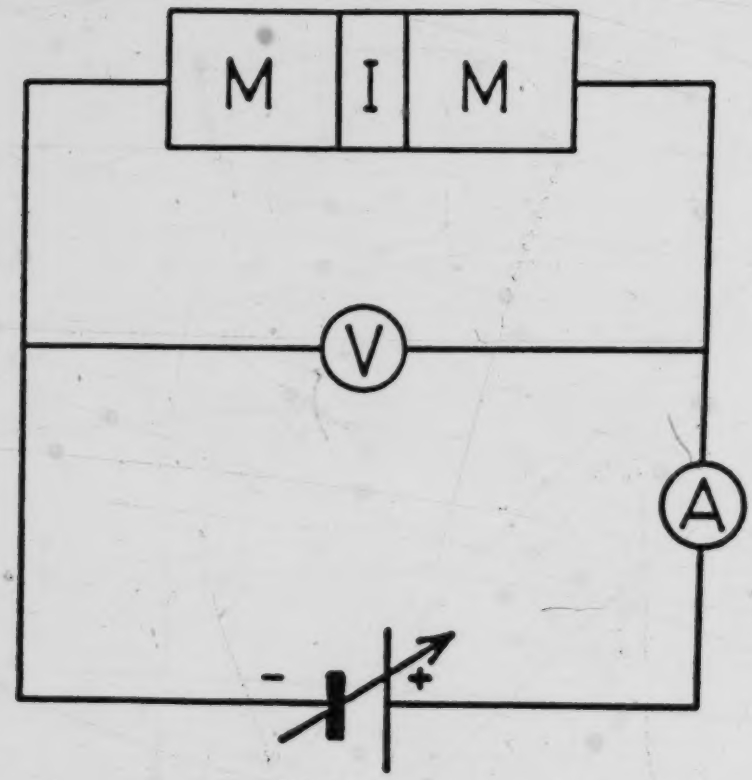

Fig. 2.1 This diagram shows the experimental arrangement for a tunneling experiment. M is a metal electrode, I is the insulating barrier, V a voltmeter and A an ammeter.

Fig. 2.2 The electron energy level diagram for a metal - insulator - metal junction is shown with and without an applied bias voltage V. Here, s is the barrier thickness, Φ_1 and Φ_2 are the barrier heights at the base and cover electrodes respectively. E_{F_1} and E_{F_2} are the Fermi levels of the two metals. When a bias is applied, tunneling occurs in the direction indicated by the arrow.

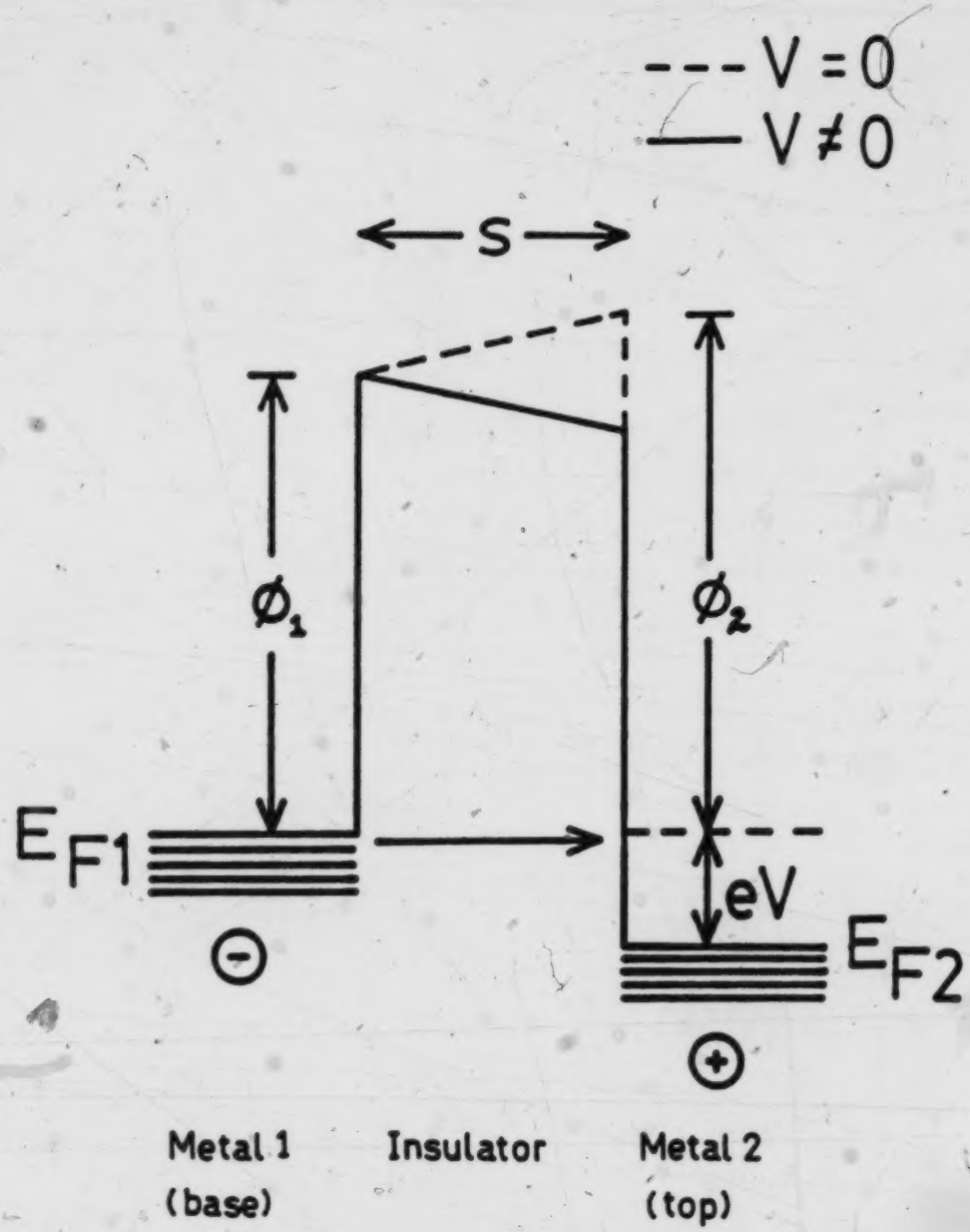
V = 0
V ≠ 0
S
Ø1
Ø2
EF1
eV
EF2
Metal 1
(base)
Insulator
Metal 2
(top)

and barrier heights Φ_1 and Φ_2 at the two electrodes.

For simplicity, we consider the zero temperature situation. At T = 0 K, all the states below E_{F_1} and E_{F_2} are filled, while those above are empty. The applied voltage V across the junction (with the left hand metal negatively biased) causes the Fermi levels to be separated by an energy eV. Filled states of metal 1 are now aligned with available empty states of metal 2 and electrons now can tunnel from the left to the right. Most of the electron tunneling occurs elastically (i. e. tunneling without change of energy), although inelastic processes, which will be discussed later, do occur. As the bias voltage V is increased, more alignment of filled states with available empty states occurs and hence, the tunneling current is increased. Therefore, depending on the bias voltage, one gets a certain current flow across the junction.

2.2 Theory of elastic tunneling

Most of the tunneling current across the junction is due to elastic tunneling in which the electron energy remains constant when it tunnels through the barrier. Harrison (Harrison 1961) has made a theoretical calculation of the elastic tunneling current based on an independent - particle model which we will describe as bellow.

According to Bardeen (Bardeen 1961), the probability per unit time for the transition of an electron from a state a in metal 1 to a state b in metal 2 on the other side of

the barrier is given by:

$$(2.1) \qquad P_{ab} = (2\pi/\hbar)|M_{ab}|^2 \rho_b f_a (1 - f_b)$$

where M_{ab} is the matrix element for the transition, ρ_b is the density of states at b, and f_a, f_b are the probabilities of occupation of states a and b respectively.

Unless the transverse wave number K_t is the same for the initial and final states the transition matrix element M_{ab} vanishes and thus ρ_b is a density of states for fixed K_t. By summing over all states a of fixed K_t to obtain ρ_a, summing over K_t, multiplying 2 for spin and e for electron charge, we obtain the total current from left to right. Subtracting the current in the opposite direction yields the current density:

$$(2.2) \qquad J = (4\pi e/\hbar)\sum_{K_t}\int_{-\infty}^{\infty}|M_{ab}|^2 \rho_a \rho_b (f_a - f_b)dE$$

with the integral over energy being taken at a fixed transverse wave number.

In the evaluation of matrix elements, states of constructed which are sinusodial in the positive energy region and drop exponentially in the adjacent negative energy region. Assuming that the band structure is uniform, except near the transition region, and also that the band structure varies only slowly in the transition region allows us to make a WKB approximation. This results in the following expression for the tunneling current density:

$$(2.3) \qquad J = 2e/h\sum_{K_t}\int_{-\infty}^{\infty}\exp(-2\int_{0}^{S}|K_x|dx)(f_a - f_b)dE$$

Where s is the barrier thickness. Note that the tunneling current density is independent of the density of states. This is a concequence of the independent - particle model.

Rewriting the wavevector K_t within the barrier region as $K(x) = 1/\hbar(2m\phi(x,V)-E)^{1/2}$ and substituting the appropriate Fermi - Dirac distribution function for f_a and f_b the current density may be written:

$$(2.4)\quad J = 2e/h\sum_{K_t}\int_{-\infty}^{\infty}\exp(-2/h\int_{0}^{S}(2m(\Phi(x,V)-E_x)^{1/2}dx)$$
$$(f(E) - f(E+eV))dE_x$$

$$f(E) = 1/(\exp(E-E_F)/K_BT + 1)$$

E_x is the total energy in the direction perpendicular to the potential barrier of thickness s and barrier heights $\Phi(x,V)$, expressed at position x and applied voltage V.

Brinkman, Dynes,and Rowell (Brinkman, Dynes and Rowell 1970) entered into this expression a trapzoidal model for the tunnel barrier:

$$\Phi(x,V) = \Phi_1 + (x/s)(\Phi_2 - \Phi_1 - eV)$$

denoting Φ_1 and Φ_2 as the barrier heights at metal 1 and metal 2. respectively with zero applied voltage and s the thickness of the barrier. By expanding (2.4) in powers of voltage and differentiating with respect to voltage, they obtained the following result for the conductance $\sigma(V)$:

$$(2.5)\quad \sigma(V)/\sigma(0) = 1 - (A\Delta\Phi/16\Phi^{3/2})eV$$

$$+ ((9/128)A^2/\Phi)(eV)^2$$

Where $\Delta\Phi = \Phi_2 - \Phi_1$ and $\bar{\Phi} = 1/2(\Phi_1 + \Phi_2)$ $A = 4\pi(2m)^{1/2}s/3h$ and $\sigma(0) = (3.16\times10^{10}\Phi^{1/2}/s)\exp(-1.025s\Phi^{1/2})$ Expression (2.5) provides a means of obtaining the barrier parameters s, Φ_1 and Φ_2 from the experimental measurement of $\sigma(V)$.

Replacing the sum over K_t in (2.4) by an integral over the projection of a constant energy surface onto the plane of the barrier i.e. $dS = 2\pi K_t dK_t$, using $\hbar k_t^2 = E_t$ and rearranging factors, we get the following expression:

$$(2.6) \qquad J = 4\pi em/h^3 \int_0^{\infty} dE_t \int_0^{E_m} \exp(-2/h \int_0^{S} (2m\Phi(x,V)-E_x)^{1/2}dx)$$
$$(f(E)-f(E+eV))dE_x$$

Tunneling experiments are often carried out at liquid helium temperature so we can make zero temperature assumption without losing generality. At T = 0 K, assumming a trapezoidal barrier (Simmons 1963), the tunneling current density J can be written as the following:

$$(2.7) \qquad J = 4\pi em/h^3 (V \int_{eV}^{E_F} p(u)du + \int_0^{eV} up(u)du)$$
$$p(u) = \exp(-As/(\Phi_2-\Phi_1-eV)((\Phi_2+u-eV)^{3/2}-(\Phi_1+u)^{3/2}))$$

Where $A = 4\beta/h(2m)^{1/2}$ and β is a correction factor which can be chosen as unity for V less than Φ_2/e.

This again provides a means of obtaining the barrier parameters (Simmons model) by fitting (least squares) the experimental I-V characteristics with this theoretical

approximation (Simmons 1963).

2.3 Theory of inelastic tunneling

Tunneling which involves a loss of electron energy during the tunneling process is called inelastic tunneling. The first report of inelastic tunneling from a loss of energy to an excitation in the barrier was by Jaklevic and Lambe (Jaklevic and Lambe 1966). In studing Al - Insulator - Pb tunnel junctions, they noticed increases in the conductance of the junction at characteristic voltages corresponding to vibrational frequencies $\hbar\omega$ of molecular species contained in the barrier region. The energy level diagram shown in Fig. 2.3 provides one with a visualization of how such processes can lead to increases in conductance.

Fig. 2.3 represents the energy diagram of a tunnel junction where the Fermi levels of the two metal electrodes (normal) are separated by an energy eV where V is the applied bias voltage. For simplicity we assume that the system is at T = 0 K which means that the states below the Fermi levels are filled while those above are empty. Electrons may tunnel elastically from metal 1 to metal 2 (process a). If a new mechanism arises which allows an electron to lose energy $\hbar\omega$ as a result of an excitation in the barrier during the tunneling process (process b), a new channel will open up. This channel is available only if there exist empty states in metal 2 which have an energy $\hbar\omega$ less than E_{F1}. This becomes possible when $eV \geq \hbar\omega$.

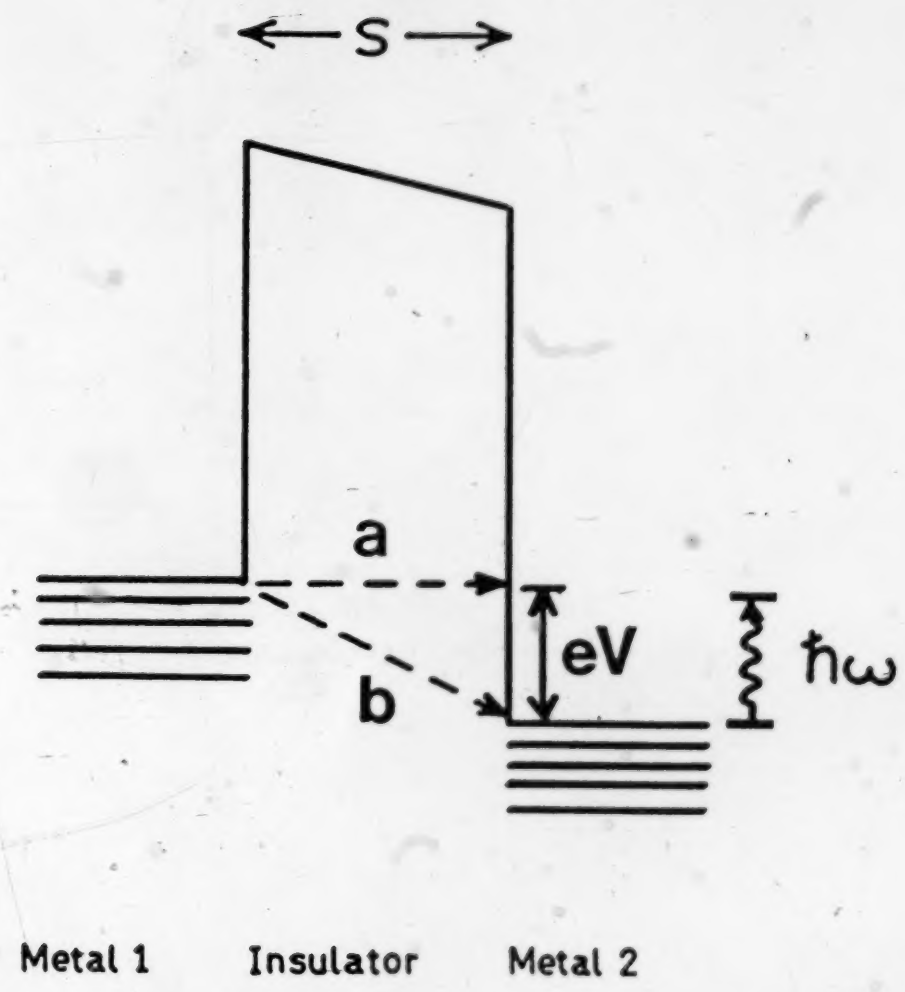

Fig. 2.3 Schematic energy level diagram for tunneling between two normal metals. a: elastic tunneling. b: inelastic tunneling. $\hbar\omega$ is the energy an electron loses to an excitation during the inelastic tunneling process b.

This onset of a new tunneling channel results in a step - like increase in the conductance and a δ function - like structure in the derivative of the conductance with respect to the voltage, as illustrated in Fig. 2.4.

At a finite temperature, the Fermi surface of both metals will smear the δ function - like structure although it will still be centered around $eV = \hbar\omega$. The excitations to which the tunneling electrons lose energies can arise from many different sources. Typical among these are the excitation of phonons of the tunnel barrier and electrodes, surface plasmons, magnons and molecular vibrations of localized impurities.

Much theoretical work on inelastic electron tunneling has been developed since Jaklevic and Lambe first discovered the phenomena in 1966. Here we briefly describe the first theoretical approach to the interaction of tunneling electrons with a molecular vibrational mode leading to an inelastic tunneling process. This approach by Scalapino and Marcus (Scalapino and Marcus 1967) is based on a simple one electron picture in which the tunneling electrons interact with the dipole field (including its image part) of a molecule in the barrier region, near the insulator -metal interface.

Taking into account the nearest image of the dipole, the electron - dipole interaction energy is, using the dipole approximation,

$$(2.8) \quad U_d = 2\exp_x/(x^2 + r^2)^{3/2}$$

Fig. 2.4 An inelastic process for a vibrational mode of frequency ω results in a break in the I - V characteristic of the tunnel junction, a step in σ vs V, and a peak in $d\sigma/dV$ vs V.

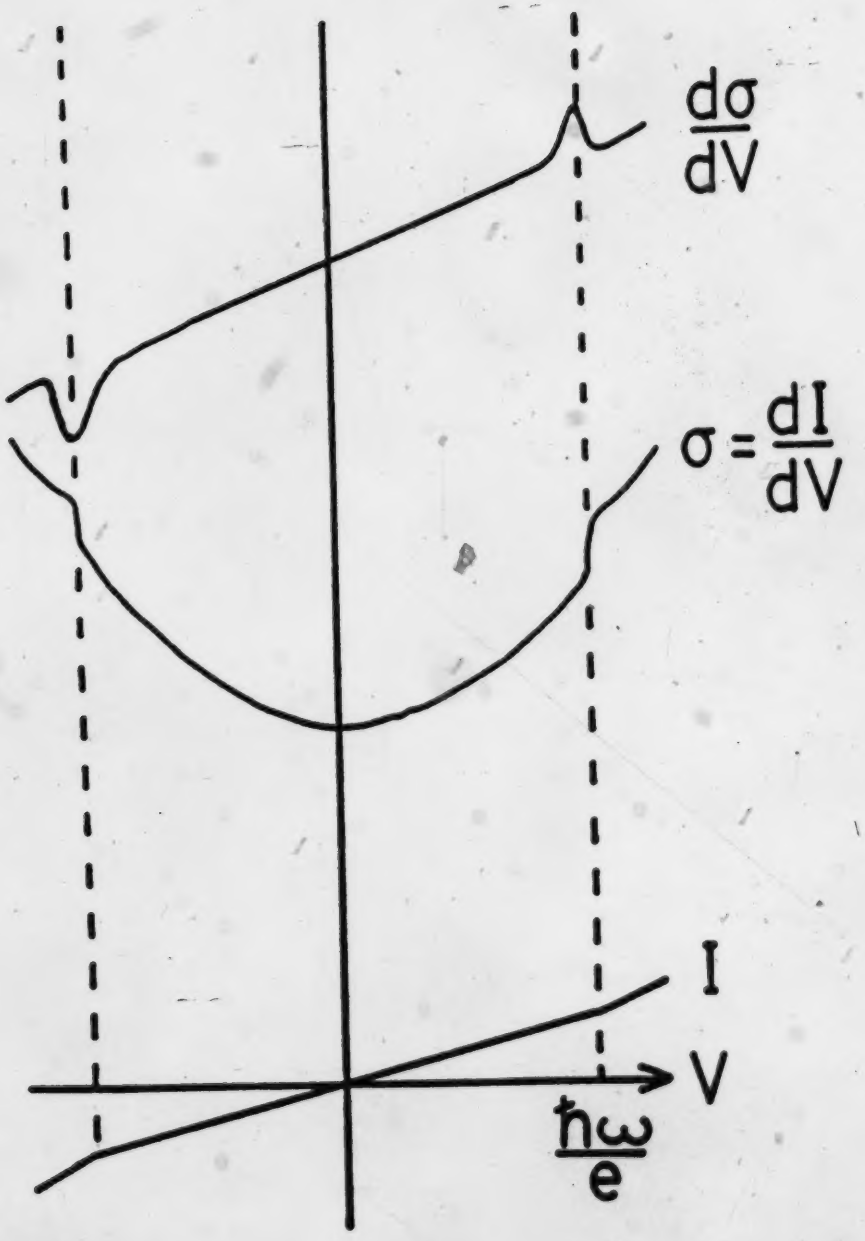
dσ/dV
σ = dI/dV
I
V
ħω/e

Where x is the distance from the metal - insulator interface to the tunneling electron (see Fig. 2.5), r is the component of the distance between the electron and the dipole perpendicular to the electron's motion, p_x is the component of the dipole moment normal to the electrode, and e is the electron charge. Using a WKB approximation for the tunneling matrix element and the "Golgen Rule" (Scalapino ans Marcus 1967), we get the second derivative of tunneling current with respect to voltage due to an inelastic process as:

$$(2.9) \qquad d^2I/dV^2 = n(4\pi e^2 m/F)\ln|s/r_o|(dI/dV)_o \Sigma|\langle m|\rho_x|0\rangle|^2\delta(V-\omega_{mo})$$

Integrating (2.9) over a voltage increment of a vibrational band yields an intensity or conductance change as:

$$(2.10) \qquad n(dI/dV)_o\ln|s/r_o|(4\pi e^2 m/F)(e^2 f_i/2m\omega_i)A$$

Where $A = \sin^2\theta$ for bending mode and $A = \cos^2\theta$ for stretching mode, ω_i and f_i are the frequency and oscillator strength of the i^{th} band, θ is the angle between the dipole and the normal to the surface, s is the thickness of the barrier, n is the number of dipoles per unit area of junction, F is the barrier height measured with respect to the energy of the tunneling electron ($F = \Phi - (E - E_F)$), and r_o is a cutoff in the vicinity of the dipole where the approximation for the potential begins to fail. For typical values of ω, f, s/r_o, F and θ, (2.10) gives a change in

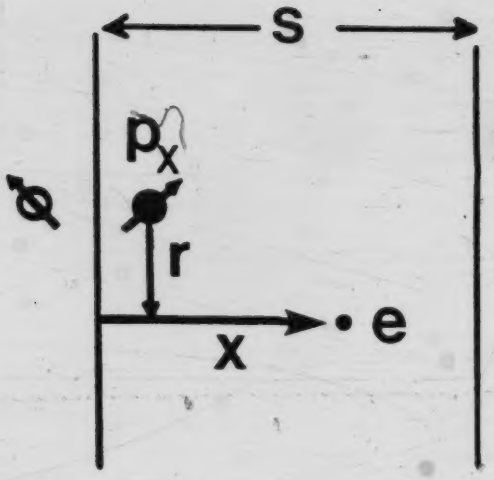

Fig. 2.5 In Scalapino and Marcus' theory, a point dipole and its image are located close to one metal electrode. The component of the dipole normal to the surface adds to its image while the component parallel to the surface cancels. The tunneling electron penetrates the barrier a distance r from the dipole and a distance x from the image plane.

conductance on the order of 0.1% consistent with experimental results.

3. EXPERIMENTAL TECHNIQUES

3.1 Junction preparation

Tunnel junctions were formed by first evaporating a set of circular indium or silver contacts onto a clean glass substrate (see Fig. 3.1). Following this, a Mg base layer (2000 A thick) was evaporated. This film was oxidized in one of the two different environments and a cover electrode subsequently evaporated.

The substrate was prepared by cutting a piece of Pyrex microscope slide 1x1 cm square, scrubbing with detergent rinsing with hot water followed briefly by methanol. A clean substrate was then flame polished and placed in a substrate holder in the vaccum chamber. The substrates were further cleaned in the vacuum chamber by exposing them to a plasma glow discharge first of oxygen then followed by argon each for 5 minutes. The size of the substrates allowed us to fabricate two junctions with a common base layer (Mg) without breaking the vacuum.

The Mg film was evaporated from a resistively heated tubular covered boat, through a stainless steel defining mask at a rate of 20 Å/s to a thickness of 2000 Å onto the substrate. The cover electrode material was evaporated from either a resistively heated boat or from a coil depending on the metal used. The boats or the coils were mounted on a

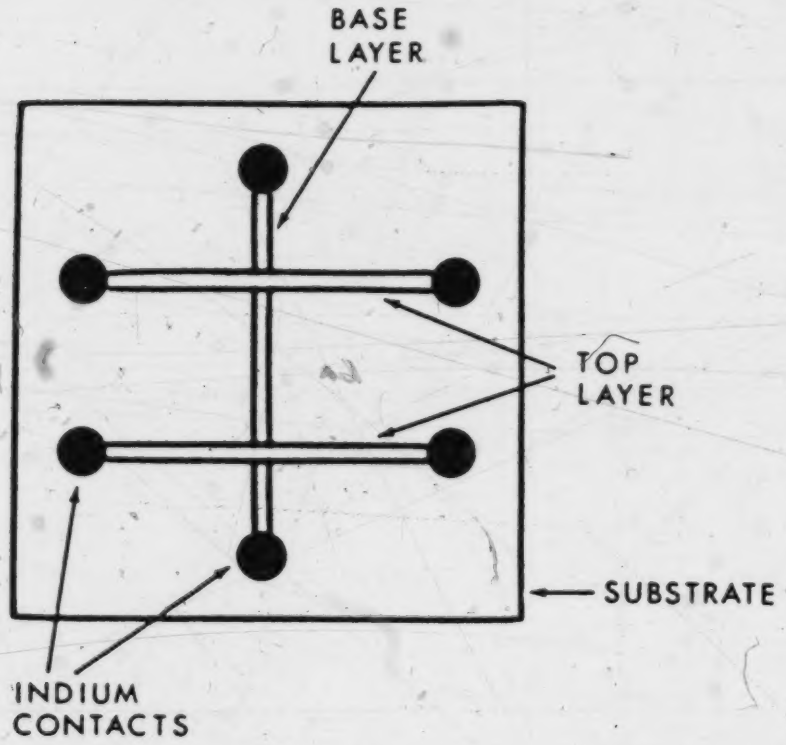

Fig. 3.1 The tunnel junction layout.

rotating carousel which allowed a proper indexing of the evaporated material. Cylindrical quartz chimneys placed around each source prevented mutual cross - contamination of metals. The metals used as cover electrodes of the tunnel junctions are listed along with the nature of the evaporation source in Table 3.1.

The vacuum chamber was pumped by an oil diffusion pump equipped with a liquid nitrogen cold trap backed by a mechanical pump. A zeolite trap was installed between the mechanical pump and rest of the system. The system was ready for the evaporation after 4 hours of pumping achieving a pressure in the low 10^{-7} torr range.

3.2 Formation of tunnel barriers

The vacuum system was equipped with a large Meissner trap located close to the substrates. The trap has an active area of $10^4 cm^2$ and was operated at 77 K. Before activation of the cold trap, the system pressure is in the 10^{-7} torr range with a partial presure of water close to $1x10^{-7}$ torr. This is referred to as the wet environment. After activating the trap, the partial presure of water drops to the 10^{-9} torr range and this situation is referred to as the dry environment.

The formation of the barriers was carried out in two different ways. For plasma junctions, the barrier was formed in the wet environment by oxidizing the freshly evaporated Mg film in a plasma glow discharge of ultra pure oxygen with

TABLE 3.1

Evaporation Materials

Metal	Purity	Supplier	Evaporation Source
Al	59	Alfa	F6-4X.030 W coil
Ag	69	Cominco	S39-.005 Mo boat
Au	69	Cominco	B12B 3x025 W basket
Cd	69	Cominco	S39-.005 Mo boat
Cu		Electrolytic tough pitch wire	S39-.005 Mo boat
In	39	INCO America	S39-.005 Mo boat
Mg	59	Johnson Matthey	S17B-.005 Ta covered boat
Pb	69	Cominco	S39-.005 Mo boat
Sn	59	Cominco	S39-.005 Mo boat
Zn	69	Cominco	S39-.005 Mo boat

Evaporation sources supplied by R. D. Mathis company.

a pressure of 200 mTorr. The ion current for this plasma glow discharge was about 13 mA, while the voltage was maintained at about 450 V and time required varied from 10 to 20 min. For gun junctions, the tunnel barrier was formed in the dry environment. In this case, the cold trap was activated 20 min. prior to the evaporation of the Mg base layer, and was kept cold until the end of the fabrication procedure. The freshly evaporated Mg film was exposed to a flux of hydrogen ions from a saddle-field ion gun for 3 to 5 min. The ion current was 0.35 mA. and a dynamic pressure of approximately 1.2×10^{-5} torr of hydrogen was maintained. After the pretreatment of hydrogen ions, the Mg film was oxidized in a plasma glow discharge of oxygen with similar parameters as for plasma junctions for 8 to 10 min.

3.3 Film thickness determination

The thickness of films during vacuum deposition was monitored by a Sloan DTM-3 quartz crystal monitor. The measurement utilizes the principle that the resonance frequency of a piezoelectric crystal depends on the mass of material deposited on the surface of the crystal (Eschbachand and Kruidhof 1965). The monitor therefore consists of a crystal placed adjacent to the substrate onto which the film is deposited, and the electric equipment for measuring the change in its resonance frequency. Eq. (3.1) relates the thickness of the deposited film to the measured frequency shift Δf (Steckelmacher 1965):

$$t = c_1 c_2 \Delta f/\rho = c\Delta f/\rho \qquad (3.1)$$

$$c = c_1 c_2$$

c_1 is a constant dependent on the thickness and cut of the piezoelectric crystal, c_2 depends on the geometry of the distribution of the deposit over the crystal and ρ is the density of the material. The validity of (3.1) is restricted to mass deposits which are at most 5% of the mass of the crystal itself (Stockbridge 1966). For all practical purposes, this condition was satisfied. In practice, c/ρ is normally calibrated experimentally by combining the shift in the resonance frequency of the crystal with a optical thickness measurement such as a Tolansky interfrometer (Tolansky 1960).

3.4 Measurement of tunneling characteristics

A system using a combination of harmonic detection and a bridge technique (Adler and Jackson 1966; Adler 1982) suitably interfaced to an on-line mini - computer facility for analog and digital recording was used to obtain the relevant information on the tunnel junctions. These are the dynamic conductance $\sigma = dI/dV$ and its derivative $d\sigma/dV$. To understand the principle of harmonic detection method, we should start with Fig. 3.2.

In this circuit the tunnel junction serves as one arm of an AC wheatstone bridge, the other arm being a variable

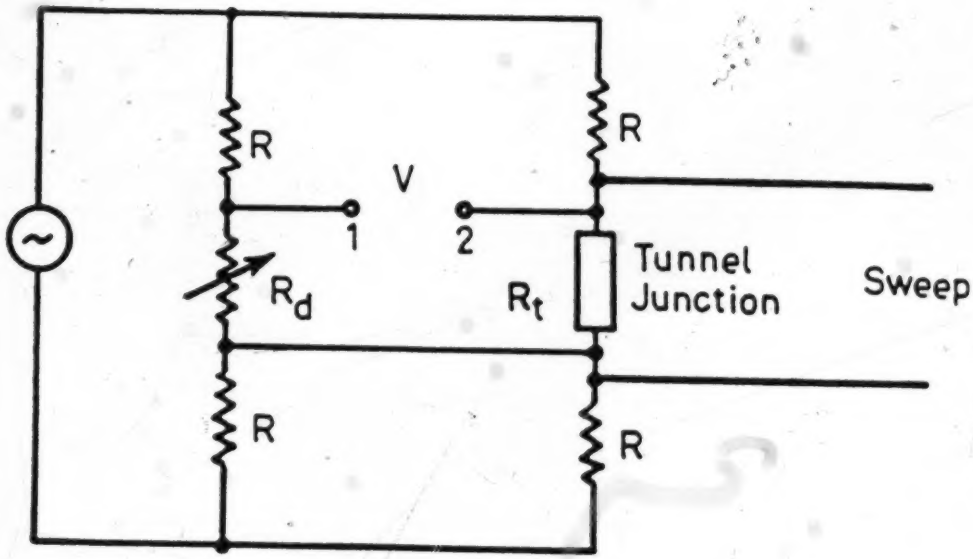

Fig. 3.2 Layout of the bridge mearsuring system.

resistor R_d. Assuming that the bridge is close to its balance and the current through each of its arms is nearly identical. In the voltage region where the tunnel junctions are investigated, they behave as weakly nonlinear passive elements. If a small current modulation is applied with the amplitude u kept constant, then the voltage V across the junction can be written in terms of Taylor's series:

$$(3.2) \quad V(I) = V(I_o) + (dV/dI)_{I_o} u\cos\omega t + 1/2(d^2V/dI^2)_{I_o} u^2\cos^2\omega t + \ldots\ldots$$

or

$$(3.3) \quad V(I) = V(I_o) + (dV/dI)_{I_o} u\cos\omega t + 1/4d^2V/dI^2)_{I_o} u^2(1 - 2\cos\omega t) + \ldots\ldots$$

Where $V(I_o)$ is the DC - bias across the junction and ω is the modulating angular frequency. The voltage across the variable resistor R_d which has a linear I - V characteristics is given by:

$$(3.4) \quad V = (I_o + u\cos\omega t)R_d$$

Thus the potential difference between point 1 and point 2 in the circuit V_{12} has components at the fundamental frequency ω and its various harmonics. The signal at the fundamental frequency, $V_{12}(\omega)$, is proportional only to the departure of the dynamic resistance (dV/dI) from R_d. Both these

components are measured by means of a lock - in amplifier.

$$(3.5) \qquad V_{1,2}(\omega) = u(R_d - (dV/dI)_{I_o})\cos\omega t$$

$$(3.6) \qquad V_{1,2}(2\omega) = (1/4)u^2(d^2V/dI^2)_{I_o}\cos 2\omega t$$

A direct calibration of the dV/dI curve enables the computation of the dynamic conductance $\sigma = dI/dV$. Ideally, the second derivative $d^2I/dV^2 = d\sigma/dV$ is then calculated using the identity:

$$(3.7) \qquad d^2I/dV^2 = -\sigma^3 d^2V/dI^2$$

The presence of second harmonic distortion in the measurement system complicates the above relation and necessitates the use of a somewhat different numerical method to calibrate $d\sigma/dV$. The details of this are described in the reference by Adler and Straus (Adler and Straus 1975; Adler 1982)

Measurements of σ and $d\sigma/dV$ as a function of voltage were made at 4.2 K using an updated version of a bridge and computerized data acquisition system (Adler and Jackson 1966; Adler 1982). The measurements were made over the range +/- 500 mV. with a modulation of 3 to 5 mV peak to peak. The σ and $d\sigma/dV$ were all calibrated, recorded, and analyzed using an on line computer system similar to the one described by Adler (Adler 1982). To allow comparison between various junctions all spectra are presented in terms of the logarithmic derivative $(1/\sigma)(d\sigma/dV)$.

4. DATA ANALYSIS

4.1 Introduction

In this chapter, the extraction of basic information from the tunneling experiment data will be discussed. Topics include peak identification in $d\sigma/dV$, the IET spectrum, determination of barrier parameters and the intensities of IET peaks.

4.2 Peak assignments

The assignment of vibrational modes due to certain molecular groups, on the basis of energy at which peaks occur in the IET spectrum is generally accomplished by comparing the IET spectra with Raman and infrared spectroscopic data, or with a theoretical calculation combined with knowledge of barrier formation. For the convenience of the following discussion, spectra of plasma and gun junctions with a Pb cover electrode are presented in Fig. 4.1.

The peak which occurs at about 450 meV in both plasma and gun junctions is assigned to the O-H stretching mode of hydroxyl groups located close to the cover electrode (Jaklevic and Lambe 1966; Lambe and Jaklevic 1968). The source of the O-H groups in plasma junctions was mainly the residual water in the vacuum chamber which was ionized

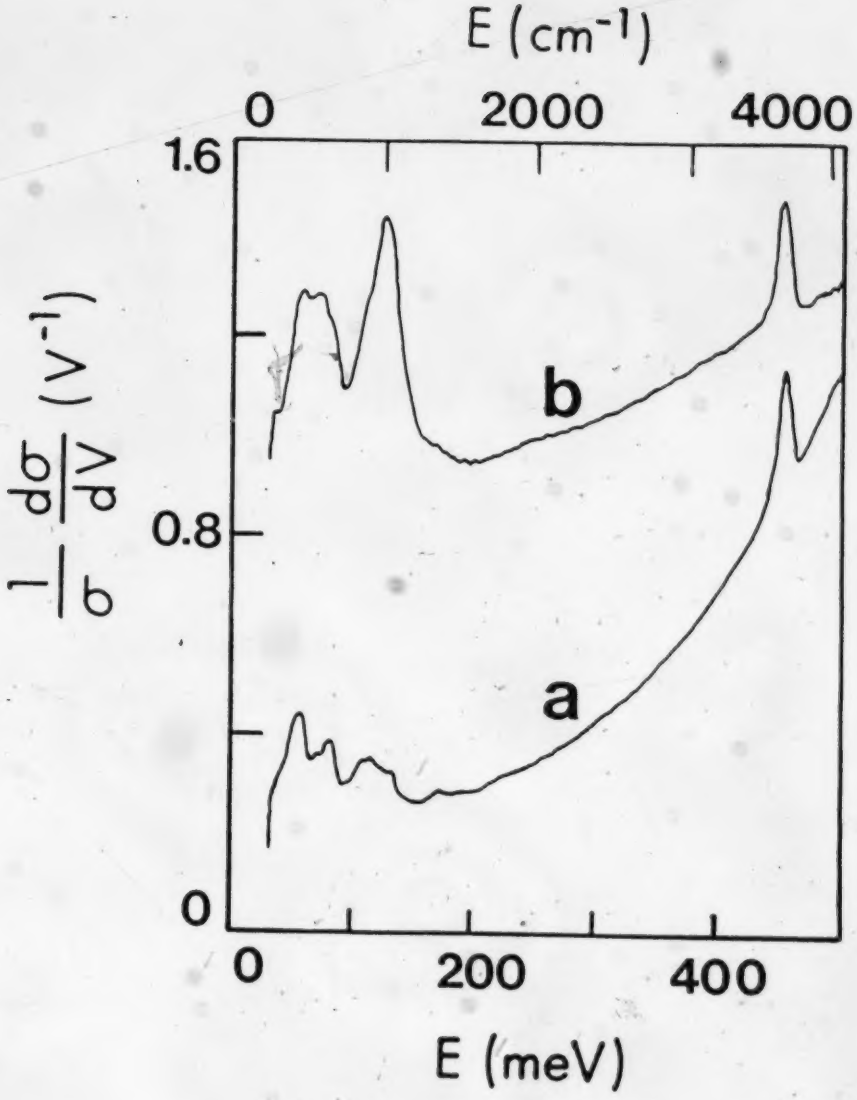

Fig. 4.1 Spectra of a plasma junction (a), and a gun junction (b) with a Pb cover electrode.

during the plasma glow discharge. For gun junctions, some of the O-H groups were generated by the combination of hydrogen provided during the hydrogen ion - pretreatment of Mg film with the oxygen used in plasma glow discharge. Values for the O-H stretching via infrared data (Silverstein and Bassler 1967) for "free" hydroxyl group in alcohols and phenols are given as 445 to 453 meV. Infrared absorption data for $Mg(OH)_2$ was also reported by Buchanan et al. (Buchanan, Caspers and Murphy 1963) and Dawson et al. (Dawson Hadfield and Wilkinson 1973) in which both stated that the O-H stretching mode is generally centered around 453 to 459 meV. Values of the O-H stretching energies measured by IETS experiments with Al - Al Oxide Metal junctions (Dragoset, Philips and Coleman 1982; Kirtley and Hansma 1975) and Mg - MgO -Metal junctions (Klein, Leger, Belin and Defourneau 1973; Plesiewicz and Adler 1986) generally agree with each other and are centered around 450 meV with the exact position depending on both the cover electrode used and the sweep polarity. we will discuss both in Chapter 5.

According to Gallagher, Ning and Adler (Gallagher, Ning and Adler 1987), the large peak occurring at 124 meV in gun junctions is due to chemisorbed hydrogen at subsurface sites on the Mg film. Hjelmberg has made theoretical estimates for the chemisorption of atomic hydrogen on the Mg(0001) surface (Hjelmberg 1979). Two stable sites were found, one on the surface, and the other subsurface. The calculated

vibrational energies of the surface site is 80 meV while that of the subsurface site is 140 meV. These calculations assume a rigid lattice and relaxation effects would lower these energies somewhat. The energy of diffusion to the subsurface sites is quite low making them relatively easy to populate. In the spectra of our gun junctions no peak near 80 meV was found attributable to the hydrogen so the peak near 124 meV was assigned to the stretching mode of hydrogen chemisorbed at subsurface sites on the Mg surface. Strong evidences in support of this assignment are the low barrier height at the Mg base electrode in gun junctions and the invariance of the 124 meV peak with various cover electrodes.

The lower portion (below 90 meV) of the spectra in plasma and gun junctions, despite the differences in peak intensities, are generally the same. The assignments of these peaks have been discussed in detail by Plesiewicz and Adler in their earlier work on MgO barriers (Plesiewicz and Adler 1986). The peaks located at 83 and 69 meV were assigned to surface phonons of the MgO barrier while the maximum at 54 meV was a combination of a surface phonon mode and the O-H bending mode of the absorbed O-H groups.

4.3 Barrier parameters

The parameters for a trapezoidal barrier can be obtained by fitting the Simmons model or the Brinkman, Dynes and Rowell (BDR) model as mentioned earlier in Chapter 2.

The fitting range is +/- 500 meV. The region between +/- 20 meV (+/- 30 meV for Pb) was avoided on account of large structures due to both the electrode phonons and zero bias anomalies. From the Simmons or BDR model, the barrier parameters which can be obtained are:

s: average barrier thickness of the trapzoidal barrier.

Φ_1: barrier height on the base electrode.

Φ_2: barrier height on the cover electrode.

The average barrier height Φ can be calculated by averaging Φ_1 and Φ_2. Since the difference between barrier parameters obtained from these two models is not great we use the parameters from the Simmons model only.

4.4 Peak intensity

The last quantities of interest are the areas under the peaks in the IET spectrum ($d\sigma/dV$), referred to as peak intensities. From the calibrated data, the peak intensity is calculated by the following integration:

$$(4.1) \qquad F(V) = \int_{V_1}^{V_2} ((1/\sigma)d\sigma/dV - g(V)\ )\ dV$$

Where g(V) is an arbitrarily chosen smooth background under the inelastic peak. V_1 and V_2 are the lower and upper bounds of the "band" (peak). In general, g(V) can be a polynomial fit but normally a straight line is adequate.

The quantity F(V) is a measure of the increase in tunneling conductance arising from the inelastic channels

opened at voltage V. From this quantity, information about the number of impurities giving rise to a peak and the coupling strength of the impurities and tunneling electrons can be estimated although it is impossible to separate out the two effects.

5. RESULTS AND DISCUSSION

5.1 Introduction

In this chapter, some of the effects of the cover electrode and the preparation techniques on the tunnel barrier parameters and the IET spectra will be presented. Interpretation of the experimental data based on simple models will be given along with discussions of possible mechanisms behind some observed anomalies.

5.2 Barrier parameters

Barrier parameters of both plasma and gun junctions with various cover electrodes are shown in Table 5.1. (the barrier parameters of a plasma junction with an Al cover are from only a single junction and may not be taken as typical values, however, it does fit the plot 5.2 nicely) From this table one can clearly see that the average barrier heights Φ are generally similar in plasma and gun junctions. The most prominent difference in barrier parameters between the two types junctions is the large barrier asymmetry in gun junctions having a lower Φ_1 and higher Φ_2. O-H dipoles absorbed near the oxide - cover interface can cause asymmetry in the tunnel barrier (Igalson and Adler 1983; Dragoset, Philips and Coleman 1982), In this case, however, we do not think the large asymmetry is solely due to the O-H

TABLE 5.1

Barrier Parameters

(eV)

	PLASMA				GUN			
Cover	Φ_1	Φ_2	Φ	$\Delta\Phi$	Φ_1	Φ_2	Φ	$\Delta\Phi$
Ag	1.05	8.40	4.72	7.35	0.44	8.47	4.45	8.03
Al	0.64	0.95	0.80	0.31	0.93	3.06	2.46	3.06
Au	1.53	8.32	4.93	6.79	-1.62	11.39	4.88	13.01
Cd	4.83	1.17	3.00	-3.67	2.37	3.28	2.82	0.91
Cu	0.90	9.56	5.23	8.66	-0.18	10.38	5.10	10.55
In	2.59	4.53	3.56	1.94	1.44	4.73	3.09	3.30
Mg					1.39	4.55	2.97	3.16
Pb	3.21	4.82	4.02	1.61	1.06	6.40	3.73	5.34
Sn	1.13	6.61	3.87	5.48	0.54	7.47	4.00	6.93
Zn	1.92	2.50	2.21	0.58	2.25	3.03	2.64	0.78

dipoles in the barrier. Our experimental results show that the quantity of O-H dipoles in both gun and plasma junctions are similar (as we will show in the following section). In a previous publication (Gallagher, Ning and Adler 1987), we have clearly demonstrated that pretreatment of the Mg film with hydrogen ions forms subsurface Mg-H bonds at the MgO interface creating a dipole layer with dipoles pointing away from the Mg surface. Physically, this dipole layer will lower the barrier height on the Mg base electrode (Igalson and Adler 1983) and make the tunneling conductance more asymmetric (Brinkman, Dynes and Rowell 1970).

The negative Φ_1 and extremely high Φ_2 in gun junctions apparent with Au and Cu cover electrodes are clearly unphysical and are due to the fact that the Simmons and BDR models are incapable of dealing with highly asymmetric conductance curve.

Looking at the trends in the average barrier height Φ with various cover electrodes we find that the average barrier height Φ increases with the ionic radius of the cover electrode for both plasma and gun junctions, as shown in Fig. 5.1. The tunnel barrier formed by native oxides is patchy and full of pinholes and grain boundaries (Halbritter 1983; Talvacchio, Gavaler, Braginski, and Janocko 1985). The increase in the average barrier height Φ with ionic radius is due to the fact that upon the evaporation of the cover electrode, metals with smaller ionic radii may penetrate more easily into the oxide through pinholes and grain

Fig. 5.1 Plots of average barrier height Φ vs ionic radius of the cover electrode for both gun and plasma junctions. Smaller ionic radii are associated with lower barrier heights.

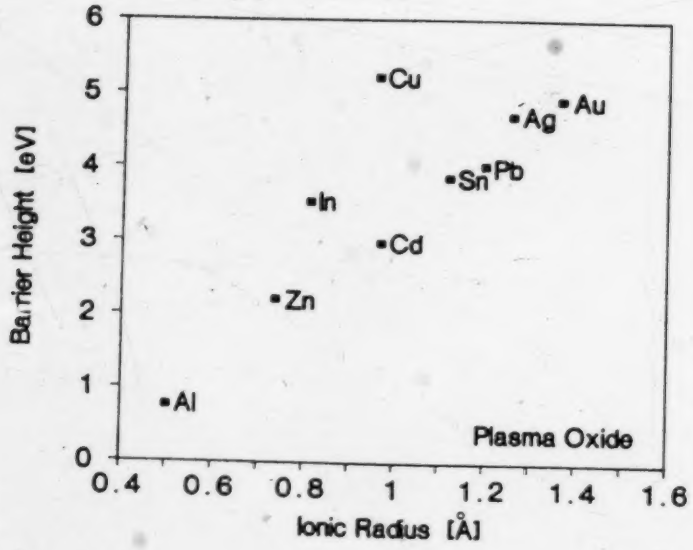
Barrier Height [eV]
Ionic Radius [Å]
Cu
Ag
Au
Sn
Pb
In
Cd
Zn
Al
Plasma Oxide
0
1
2
3
4
5
6
0.4
0.6
0.8
1
1.2
1.4
1.6

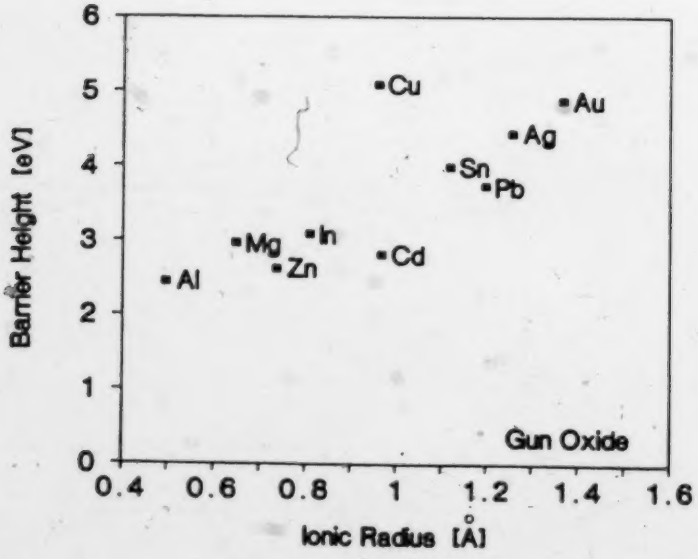
Barrier Height [eV]
Ionic Radius [Å]
Cu
Au
Ag
Sn
Pb
Mg
In
Cd
Zn
Al
Gun Oxide
0
1
2
3
4
5
6
0.4
0.6
0.8
1
1.2
1.4
1.6

boundaries and result in more effective microshorts which lower the barrier height. One may argue that the effective thickness of the tunnel barrier may also be reduced by these microshorts making the tunnel barrier obtained from the fitting program effectively lower since one cannot separate these two parameters well in paractice. The modification of the barrier thickness should not be drastic since the area of these microshorts should be very small compared to that of the junction barrier.

In Fig. 5.1, the barrier height of Cu is anomalously high. It may be due to some kind of chemical reaction between the Cu electrode and the O-H dipoles absorbed on the MgO barrier as what has been observed by Konkin and Adler (Konkin and Adler 1983). However we do not have enough evidence to make any comment or draw any conclusions at this stage of our studies.

5.3 IET spectra

The IET spectra of the two types of junctions with various cover electrodes is shown in Fig. 5.2. Absent cover metals in the spectra of plasma junctions are Al and Mg with which we have experienced great difficulties in obtaining usable junctions. All the spectral features which appear in plasma junctions are evident in gun junctions despite differences in the relative peak intensities. The unique feature in gun junctions is the large peak at 124 meV independent of the cover electrode. Both peak intensity and

Fig. 5.2 $1/\sigma(d\sigma/dV)$ for Mg - MgO - Metal junctions. (a) and (b): gun junctions. (c) and (d): plasma junctions. Al and Mg are absent in plasma junctions due to the difficulties experienced in obtaining usable junctions repeatedly.

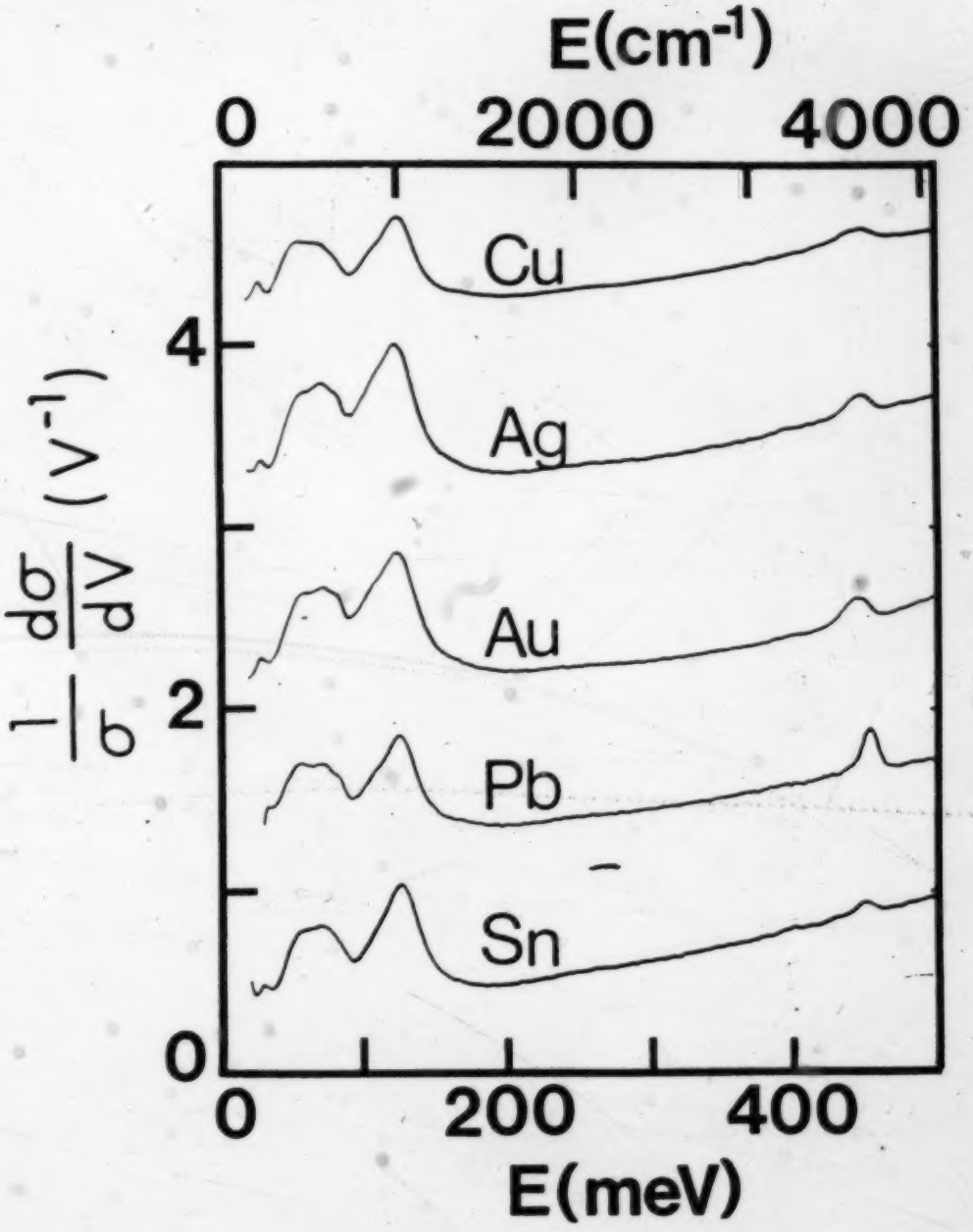

(a)

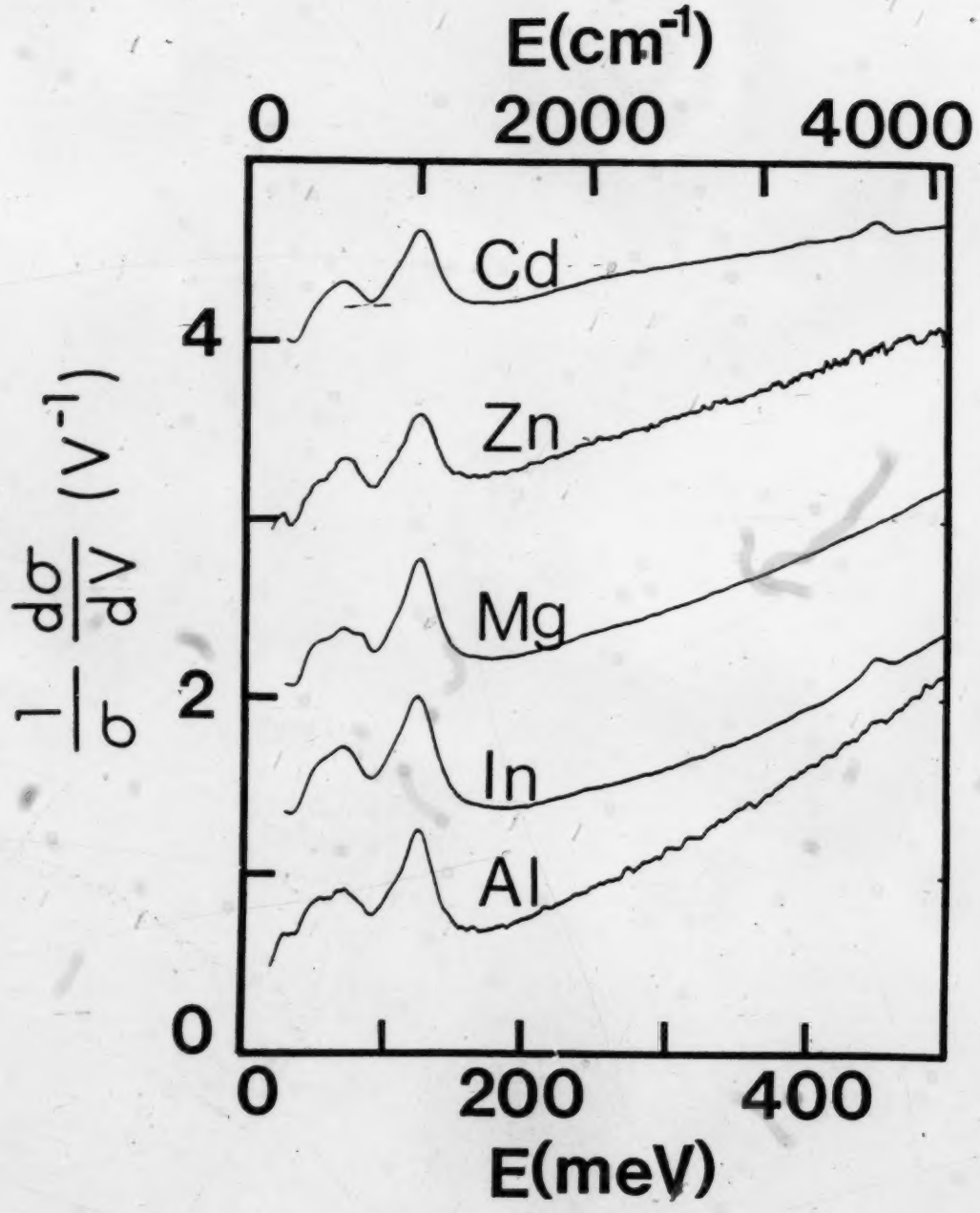

(b)

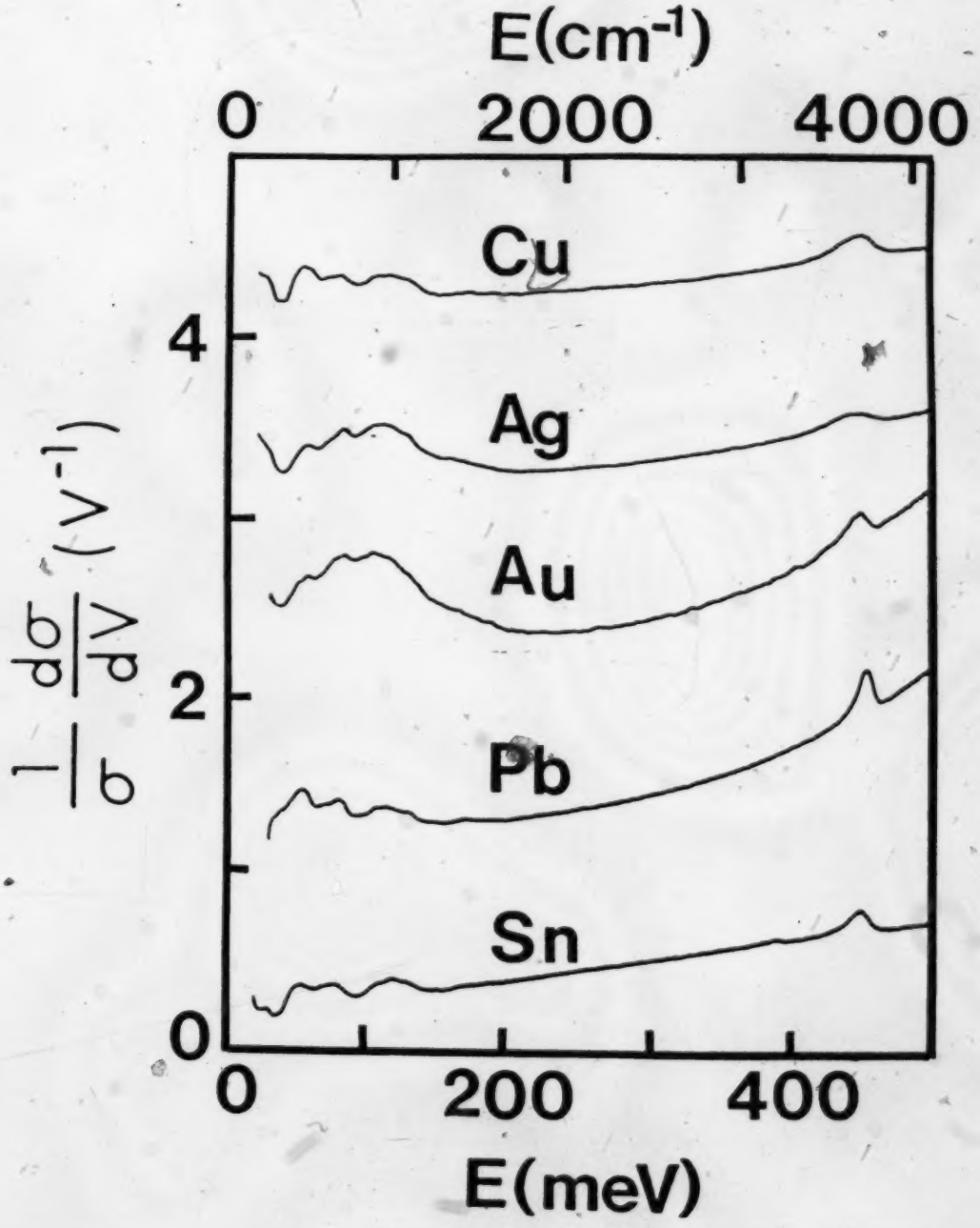

(c)

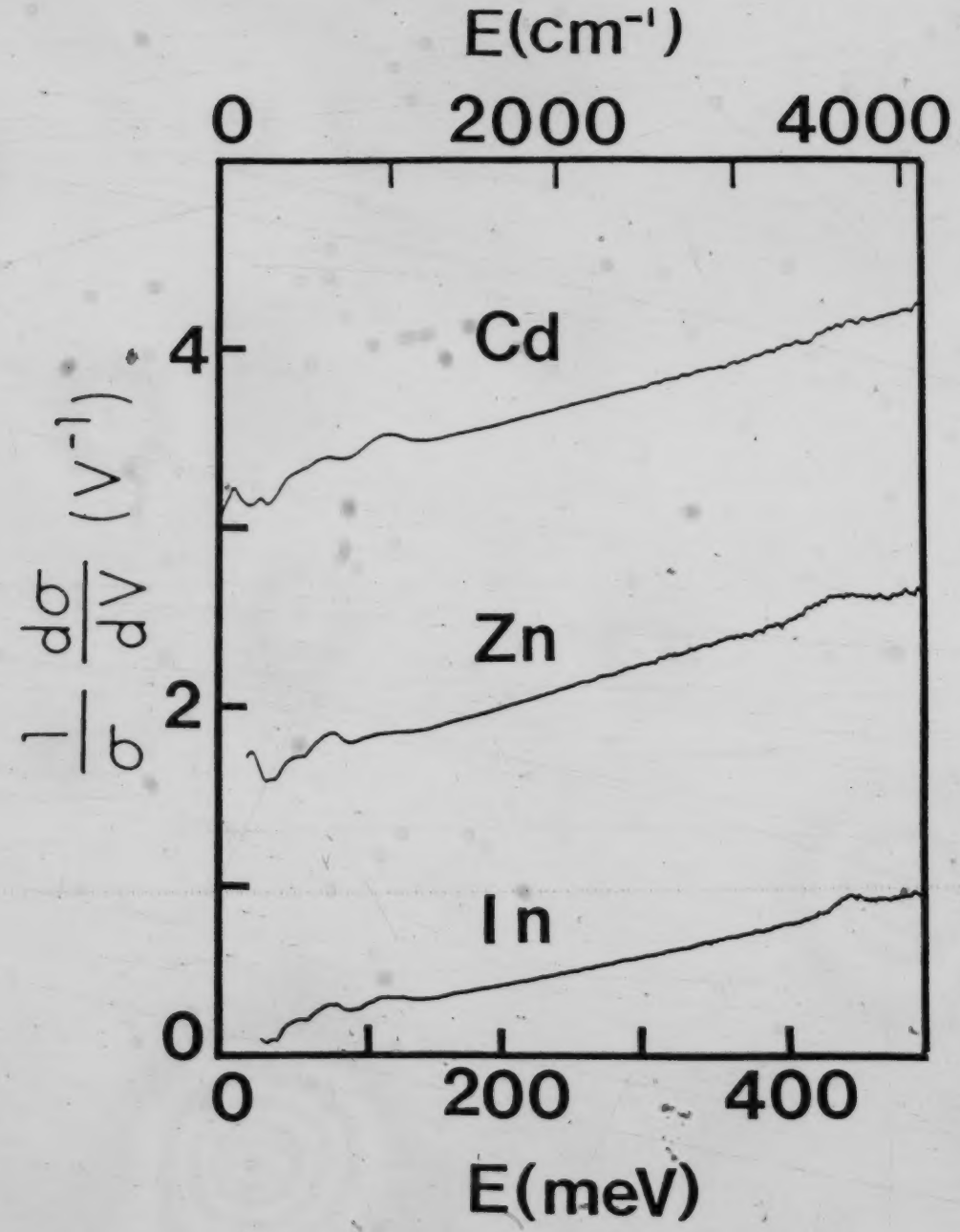
E(cm⁻¹)
0
2000
4000
Cd
Zn
In
4
2
0
$\frac{1}{\sigma}\frac{d\sigma}{dV}$ (V⁻¹)
0
200
400
E(meV)

(d)

position are relatively invariant with the various cover electrodes. The peak is assigned to the Mg-H vibrational mode (Gallagher, Ning and Adler 1987). In general, the low energy (below 200 meV) portion of the spectra in gun junctions is less influenced by the cover electrode while that of plasma junctions is modified more drastically. In the previous publication we have concluded that the pretreatment of Mg film with hydrogen ions helps to grow a more uniform amorphous - like MgO tunnel barrier which seems to be "tougher" (Gallagher, Ning and Adler 1987; Liehr and Ewert 1983; Talvacchio, Gavaler Braginski and Janocko 1985). In our simple model, we assume that the cover metal affects the oxide barrier by penetrating into the pinholes and grain boundaries of the MgO barrier, thus in gun junctions, we would expect less influence of cover metal on the spectra due to its tougher character.

5.4 The O-H stretching peak

The peak at about 450 meV is due to the O-H stretching mode (Jaklevic and Lambe 1966; Lambe and Jaklevic 1968). The peak intensities and positions of the O-H stretch mode in both plasma and gun junctions is shown in Table 5.2. The common feature is that the peak intensity is always higher on the negative side of the spectra. This implies that the mojority of electrons which tunneled inelastically losing energy to the O-H stretching modes were those which tunneled from the base to the cover electrode. Since it is more

TABLE 5.2

F(+)/F(-): Peak intensity of O-H stretching mode from positive/negative side of the IET spectra. F(avg): average O-H peak intensity between positive and negative sides of the spectra. E(+)/E(-): O-H energy from the positive/negative side of the IET spectra.

TABLE 5.2

O-H Peak Intensities and Positions

PLASMA

Cover	F(-)	F(+)	F(avg)	E(-)	E(+)
		(10^{-3})		(meV)	
Ag	2.75	1.20	1.98	442.5	452.0
Au	2.70	2.60	2.65	445.5	449.0
Cd					
Cu	3.85	2.88	3.36	447.3	449.3
In	1.90	1.30	1.60	453.5	450.0
Pb	2.80	2.77	2.79	452.6	453.6
Sn	2.72	1.58	2.15	450.2	451.0

GUN

Ag	2.10	1.60	1.85	446.9	450.7
Au	2.73	2.00	2.36	444.3	449.0
Cd	1.20	0.94	1.07	448.5	453.5
Cu	2.65	1.55	2.10	446.0	450.5
In	1.35	0.89	1.12	450.5	455.0
Pb	3.60	2.40	3.00	452.8	453.8
Sn	0.83	0.70	0.77	448.2	451.3

probable for electrons to tunnel through the barrier at high energy then undergo an inelastic process, we conclude that the concentration of O-H dipoles is higher close to the cover electrode and gradually decreases as one gets into the oxide barrier.

In addition to the peak intensity, we can also see that in both plasma and gun junctions, the peak position or the energy of this stretching mode depends on the cover electrode. As the cover metals are changed from Pb to In, Cd, Sn, Cu, Ag and Au, the energy shifts to lower values. With O-H dipoles in close proximity to the cover electrode, two possible mechanisms become apparent. The first is an image dipole effect. When a dipole oscillates in front of a metal plane, it will couple with its image and the coupling will shift the oscillating frequency (hence the energy $h\omega$) down (Motawitz 1969). According to Kirtley and Hansma's calculation (Kirtley and Hansma 1976), the frequency shift behaves in the following way:

$$(5.2) \quad \omega_o - \omega \propto q^2/(m\omega_o d^3 n^2)$$

Where q is the effective charge of the oscillating dipole, m the reduced mass, ω_o the unperturbed frequency, d the distance between the dipole and the imaging plane and n the real index of refraction of the oxide. In Fig. 5.3 we have plotted the average (between the positive and negative sides of the spectra) energy of this stretching mode against the atomic radius of the cover electrode for the gun junctions.

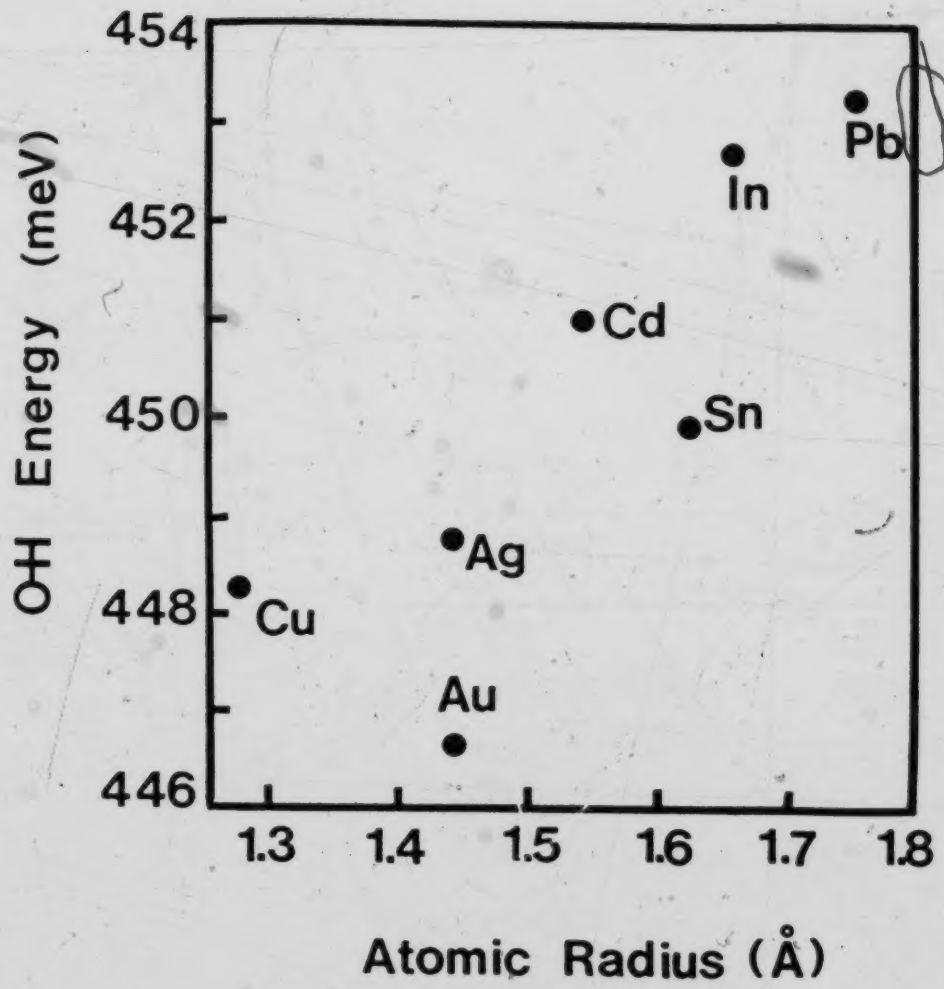

Fig. 5.3 Plot of O-H stretching energy in gun junctions vs atomic radius of the cover electrode. Lower energies (larger shifts) are associated with smaller atomic radii. The trend for plasma junctions is identical and is omitted for simplicity.

The trend in plasma junctions is identical and is omitted for clarity. What we can see from Fig. 5.3 is that the energy increases with the atomic radius of the cover electrode. This is in agreement with Kirtley and Hansma's work (Kirtley and Hansma 1975, 1976) in which they concluded that cover metals with smaller atomic radii can pack closer onto the O-H dipoles. The smaller effective distance between the imaging plane and the O-H dipoles results in a lower O-H stretching energy (larger shift).

It is not clear where the effective imaging plane is with respect to the metal surface in surface studies whenever the interaction between a charge and a metal surface is involed. According to Newns' (Newns 1969) calculation which is based on a Fermi - Thomas approximation, the effective imaging plane should be pushed back by a distance r_s with respect to the metal plane, where r_s is the Fermi - Thomas screening length. If we assume that the effective distance between the dipole and the imaging plane has two major components: r_s determined by the screening effect, d_o determined by the atomic radius, then we can write the total effective distance between the dipoles and the imaging plane d_t as the following:

$$d_t = d_o + r_s \qquad (5.3)$$

For the cover metals we used, typical values of the screening length r_s are between 0.5 and 0.6 Å, and the values for d_o from Kirtley and Hansma's calculation (Kirtley

and Hansma 1976) is around 0.6 - 0.8 Å. Using these numbers we would expect the screening effect to dominate. However, when we look at the correlation between the O-H stretching energy and the screening length of the cover metal, we find the energy shift increases with the screening length. This is in contrast to what is expected . As the screening length r, goes up, d would go up as well and result in a smaller shift in the O-H stretching energy. This is not what is seen and indicates that the screening effect is not the prime factor to consider in this case, and that Newns calculation is insufficient for this more complicated situation.

The second mechanism (Kirtley and Hansma 1975) is due to the possible hydrogen bonding between O-H group and the cover metal. Experimental results (Konkin and Adler 1979, 1980) show that the O-H dipoles are orientated with the H' close to the cover electrode. A hydrogen bond might be expected to occur between the cover electrode and the O-H dipoles. This would lower the electron density in the O-H bond decreasing the bond strength and the frequency of the stretching mode. According to Pauling's theory (Pauling 1949) of metals, the quantity to characterize the interaction strength of a metal with hydrogen is the amount of d character of the metal element. A higher percentage of d character results in stronger bonds, therefore we might expect a lower O-H stretching energy from a cover electrode with a larger percentage of d character. In Fig. 5.4 we have plotted the average O-H stretching energy versus the

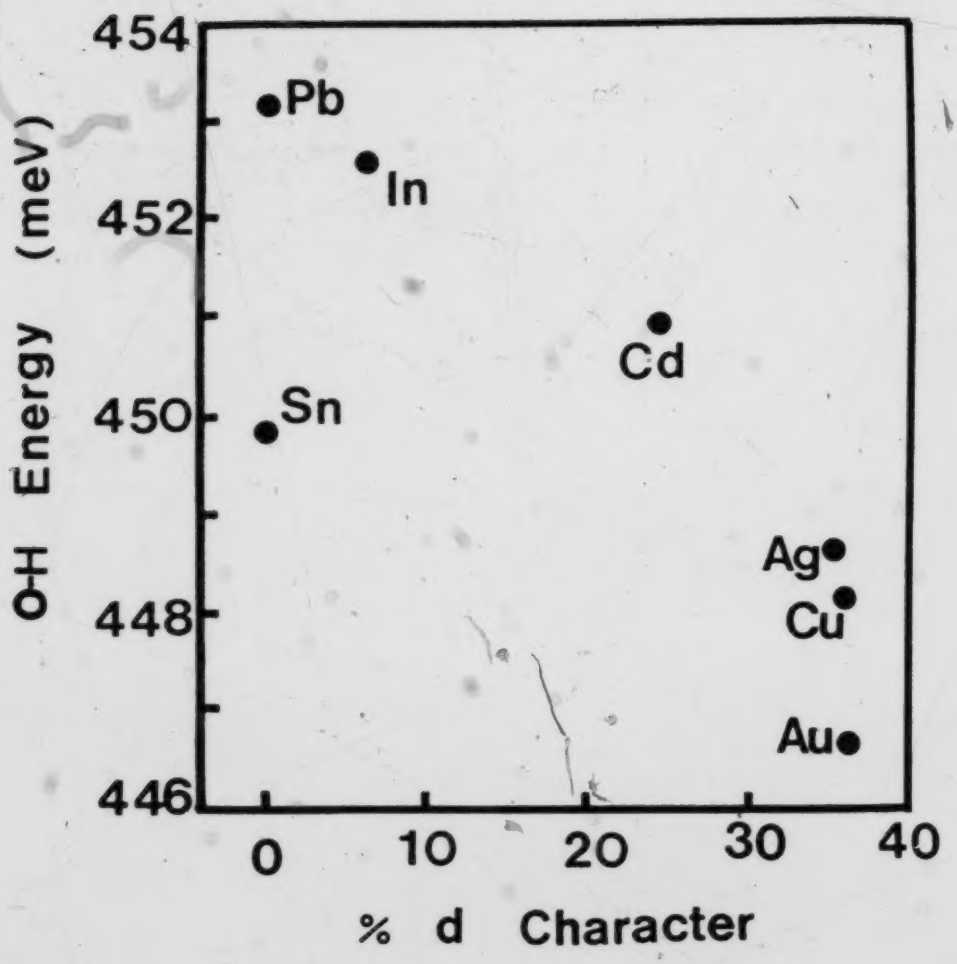

Fig. 5.4 Plot of O-H stretching energy in gun junctions vs the percentage of d character in electronic valance bands in the cover metals (from Pauling). Lower energies are associated with a larger percentage of d character. Again, plot of plasma junctions shows the same trend and is omitted for clarity.

percentage of d character of the cover metal for gun junctions (again, plot for plasma junctions is omitted for clarity). The general trend is clear and is in agreement with Kirtley and Hansma's work (Kirtley and Hansma 1975). The observed O-H stretching energy for the Au cover electrode is somewhat lower than expected according to this model, and suggests further consideration in order to reduce the scatter.

Not only does this O-H stretching energy depend on the cover electrode, it also depends on the sweep polarity. The energy is lower on the negative side of the spectra as shown in Table 5.2. The exception is plasma indium which has a small peak intensity making the position difficult to determine. The concentration of the O-H dipoles is higher close to the cover electrode and gradually decreases deep into the oxide barrier. Since the image dipole effect and the hydrogen bonding mechanism are most prominent for the O-H dipoles close to the cover electrode, the O-H stretching energy of these O-H dipoles will be lower (weaker O-H bond) than O-H dipoles deeper in the oxide. The high concentration of O-H dipoles close to the cover electrode results in a smaller average distance between the neighboring O-H dipoles. According to Lippincott and Schroeder (Lippincott and Schroeder 1955), O-H dipoles will interact with each other by hydrogen bonding between the H^+ and O^- in the neighboring dipoles. The interaction becomes more prominent as the distances between the O-H dioples get smaller and

further weaken the O-H bond strength of O-H dipoles located close to the cover electrode. Thus, we expect a weaker bond strength from the O-H dipoles close to the cover electrode. Since more O-H dipoles close to cover electrode will be excited when the electrons tunnel through the barrier from the base to the cover (corresponds to the negative side of the spectra), therefore, the O-H stretching energy measured for this polarity will be lower.

5.5 Discussion of the 124 meV peak

The peak at 124 meV is unique to gun junctions and clearly due to the chemisorbed hydrogen on Mg surface. The peak intensity and position of this 124 meV peak are indepent of cover electrode within the accuracy of the experiment, as shown in Table 5.3. All these, together with the lowering of Φ_1, indicate that the source of this peak is in the vicinity of the Mg base electrode.

TABLE 5.3

F(+)/F(-): Peak intensity of the 124 meV peak from the positive/negative side of the spectra, F(avg): average peak intensity between positive and negative sides of the spectra; E(+)/E(-): peak position from the positive/negative side of the spectra.

TABLE 5.3

124 meV Peak Intensities and Positions

Cover	F(-)	F(+)	F(avg)	E(-)	E(+)
		(10^{-3})		(meV)	
Ag	14.7	14.3	14.5	124.5	122.7
Al	11.8	14.1	13.0	124.5	125.8
Au	13.2	13.3	13.2	122.3	124.5
Cd	12.5	13.0	12.8	124.0	126.0
Cu	13.3	12.5	12.9	124.3	124.9
In	15.0	14.0	14.5	122.3	125.3
Mg	14.0	15.7	14.8	124.5	125.0
Pb	14.9	13.0	13.9	123.0	124.0
Sn	11.7	13.3	12.5	124.0	125.0
Zn	12.0	13.5	12.7	125.0	126.0

6. SUMMARY AND CONCLUSION

6.1 Conclusion

We have found that both the cover electrode and the preparation method have a dramatic influence on the tunnel barrier properties and the IET spectral features. We have demonstrated that the average tunnel barrier height is very much cover electrode dependent and increases with the ionic radius of the cover electrode due to microshorts created by penetration of the cover metal into the oxide barrier. The low barrier height on the Mg base side Φ_1 and hence the large barrier asymmetry in gun junctions is clearly due to the dipole layer formed by the chemisorbed hydrogen subsurface at the Mg surface (Gallagher, Ning and Adler 1987). This hydrogen chemisorption is also responsible for the large peak at 124 meV.

In general, the spectral features of plasma junctions below 200 meV are more drastically influenced by the cover electrode while those of the gun junctions are less sensitive. This indicates the tougher character of the oxide barrier in gun junctions.

The O-H stretching energy measured from the IET spectra depends on both the cover electrode and sweep polarity regardless of the preparation technique. The unexpected high barrier height of Cu cover electrode may be related to a

chemical reaction at the oxide copper interface.

6.2 Suggestion for further work

A good deal of information has been obtained through this work while many questions remain unanswered. To gain a better insight into the role the cover electrode plays in determining the barrier properties and the effect of the cover electrode on the IET spectral features, knowledge of the tunnel barrier before evaporation of the cover metal seems essential. A similar experiment in a system equipped with surface analysis apparatus (such as a UHV system with Auger spectroscopy, LEEDS etc.) would be very informative. The effect of the substrate conditions (such as cooled substrates, roughened substrates) needs to be investigated.

The effects of hydrogen ion pretreatment of the base layer may be extended to some other base electrodes such as Pb. This experiment should be of interest since one could possibly study the localized phonon modes due to hydrogen (Nedrud and Ginsberg 1981), and in addition, this experiment may supplement the studies of hydrogen chemisorption at metal surfaces and the growth of oxide barriers carried out previously (Gallagher, Ning and Adler 1987).

BIBLIOGRAPHY

Adler J. G. and J. E. Jackson (1966)

System for observing small non-linearities in tunnel junctions. Rev. Sci. Intrum. 37, 1049 (1966)

Adler J. G. and J. Straus (1975)

Application of minicomputers in high resolution electron tunneling. Rev. Sci. Intrum. 46, 158 (1975)

Adler J. G. (1982)

Computer-assisted determination of peak profiles, intensities, and positions. in Tunneling Spectroscopy, edited by P. K. Hansma Plenum, New York, (1982), P.423

Bardeen J. (1961)

Tunneling from a many-particle point of view. Phys. Rev. Lett. 6, 57 (1961)

Brinkman W. F., R. C. Dynes and J. M. Rowell

Tunneling conductance of asymmetrical barriers. J. Appl. Phys. 41, 1915 (1970)

Buchanan R. A., H. H. Caspers and J. Murphy (1963)

Lattice vibration spectra of $Mg(OH)_2$ and $Ca(OH)_2$. Appl. Opt. 2, 1147 (1963)

Dawson P., C. D. Hadfield and G. R. Wilkinson (1973)

The polarized infrared and Raman spectra of $Mg(OH)_2$ and $Ca(OH)_2$. J. Phys. Chem. Solids, 34, 1217 (1973)

Dragoset R. A., E. S. Philips and R. V. Coleman (1982)
Effects of barrier preparation on inelastic electron tunneling. Phys. Rev. B 26, 5333 (1982)

Eschbach H. L. and W. E. Kruidhof (1965)
Vacuum Microbalance Techn. 3, 207 (1965)

Gallagher M. C., Y. B. Ning and J. G. Adler (1987)
Inelastic electron tunneling studies of the effects of hydrogen on the growth of MgO. Phys. Rev. B 36 (Oct. 15, 1987)

Halbritter J. (1983)
On resonant tunneling in Nb-Nb_2O_5-Diodes. IEEE Transactions on magnetics, Vol. Mag-19, No.3 799 (1983)

Hansma P. K. (Editor) (1982)
Tunneling Spectroscopy. Plenum New York, (1982)

Harrison W. A. (1961)
Tunneling from an independent-particle point of view. Phys. Rev. 123, 85 (1961)

Hjelmb[illegible] H. (1979)

Hydrogen chemisorption on Al, Mg, and Na surfaces-calculation of adsorption sites and binding energies. Surf. Sci. 81, 539 (1979)

Igalson J. and J. G. Adler (1983)
Effect of hydrogen-isotope implantation on aluminum oxide tunnel-junction barriers. Phys. Rev. B 28, 4970 (1983)

Jaklevic R. C. and J. Lambe (1966)
Molecular vibration spectra by electron tunneling. Phys. Rev. Lett. 17, 1139 (1966)

Kirtley J. and P. K. Hansma (1975)
Effect of the second metal electrode on vibrational spectra in inelastic-electron-tunneling spectroscopy. Phys. Rev. B 12, 531 (1975)

Kirtley J. and P. K. Hansma (1976)
Vibrational-mode shifts in inelastic electron tunneling spectroscopy: Effects due to superconductivity and surface interactions. Phys. Rev. B 13, 2910 (1976)

Klein J., A. Leger, M. Belin and D. Defourneau (1973)
Inelastic-electron-tunneling spectroscopy of metal-insulator-metal junctions. Phys. Rev. B 7 2336 (1973)

Konkin M. K. and J. G. Adler (1979)
Annealing effects in tunnel junctions (thermal annealing). J. Appl. Phys. 50, 8125 (1979)

Konkin M. K. and J. G. Adler (1980)
Annealing effects in tunnel junctions (voltage annealing). J. Appl. Phys. 51, 5450 (1980)

Konkin M. K. and J. G. Adler (1983)
Chemcal interaction of a cover metal with an oxide barrier studied by tunneling spectroscopy. J. Phys. Chem. 87, 2477 (1983)

Lambe J. and R. C. Jaklevic (1968)
Molecular vibration spectra by inelastic electron tunneling. Phys. Rev. 165, 821 (1968)

Liehr M. and S. Ewert (1983)
Inelastic electron tunneling spectroscopy on Ultrahigh vacuum prepared tunnel junctions. Z. Phys. B-Condensed Matter 52, 95 (1983)

Lippincott E. R. and R. Schroeder (1955)
One-dimensional model of the Hydrogen Bond. J. Chem. Phys. 23, 1099 (1955)

Magno R., M. K. Konkin and J. G. Adler (1977)

Effect of cover electrode metal on inelastic electron tunneling structure. Surf. Sci. 69, 437 (1977)

Motawitz H. (1969)
Self-coupling of a two-level system by a mirror. Phys. Rev. 187, 1792 (1969)

Nedrud B. W. and D. M. Ginsberg (1981)
Localized modes of oscillation in hydrogen and deuterium doped lead Physica 108 B, 1175 (1981)

Newns D. M. (1969)
Fermi-Thomas response of a metal surface to an external point charge. J. Chem. Phys. 50, 4572 (1969)

Pauling L. (1949)
A resonating-valance-bond theory of metals and intermetallic compounds. Proc. R.Soc. A, 196, 343 (1949)

Plesiewicz W. and J. G. Adler (1986)
Inelastic electron-tunneling study of MgO barriers. Phys. Rev. B 34, 4583 (1986)

Scalapino D. J. and S. M. Marcus (1967)
Theory of inelastic electron-molecule interactions in tunnel junctions. Phys. Rev. Lett. 18, 459 (1967)

Silverstein R. M. and G. C. Bassler (1967)
Spectrometric Identification of Organic Compounds. J. Wiley & Sons, Inc., New York, (1967)

Simmons J. G. (1963)
Electric tunnel effect between dissimilar electrodes separated by a thin insulating film. J. Appl. Phys. 34, 2581 (1963)

Steckelmacher W. (1965)
in Thin Film Microelectronics, ed by L. Holland, John Wiley & Sons, New York, (1965) P. 193

Stockbridge C. D. (1966)
in Vacuum Microbalance Techniques, ed by K. Behrndt, Plenum Press, New York, (1966) Vol. 5, P. 193

Talvacchio J., J. R. Gavaler, A. I. Braginski and Janocko (1985)
Artificial oxide barrier for NbN tunnel junctions. J. Appl. Phys. 58, 4638 (1985)

Tolansky S. (1960)
in Surface Microtopography Longmans Green and Co. Ltd., (1960)

Wolfram T. (Editor) (1977)

Inelastic Electron Tunneling Spectroscopy, Proceedings of the International Conference and Symposium on Electron Tunneling, University of Missouri-Columbia, USA, May 25-27, (1977)